Applied Catalysis B: Environmental 111–112 (2012) 545–554

Contents lists available at SciVerse ScienceDirect

Applied Catalysis B: Environmental

journal homepage: www.elsevier.com/locate/apcatb

Mild solar photo-Fenton: An effective tool for the removal of *Fusarium* from simulated municipal effluents

M. Inmaculada Polo-López[a], Irene García-Fernández[a], Theodora Velegraki[b], Athanasia Katsoni[b], Isabel Oller[a], Dionissios Mantzavinos[b], Pilar Fernández-Ibáñez[a,*]

[a] *Plataforma Solar de Almería – CIEMAT, P.O. Box 22, 04200 Tabernas, Almería, Spain*
[b] *Department of Environmental Engineering, Technical University of Crete, Polytechneioupolis, GR-73100 Chania, Greece*

ARTICLE INFO

Article history:
Received 16 September 2011
Received in revised form 25 October 2011
Accepted 1 November 2011
Available online 7 November 2011

Keywords:
Solar disinfection
Fusarium solani
Mineralization
Wastewater
Competition

ABSTRACT

In this work, the efficacy of natural solar radiation (up to 21.1 kJ/L of UV energy dose) combined with homogeneous iron (5 and 10 mg/L Fe^{2+}) and/or hydrogen peroxide (10 and 20 mg/L) to treat a simulated municipal effluent in a solar bottle reactor was assessed. Emphasis was given on the inactivation of resistant spores with *Fusarium solani* serving as the test species in a matrix containing 25 mg/L of dissolved organic carbon, 65 mg/L of inorganic carbon and pH about 8. Processes like dark Fenton oxidation (5 mg/L Fe^{2+} and 10 mg/L H_2O_2 at pH 3), solar radiation alone (at 21.1 kJ/L and pH 3–8) and H_2O_2 oxidation alone (up to 20 mg/L in the dark) led to no or inadequate disinfection, thus showing the resistance of *F. solani*. Solar irradiation in the presence of 10 mg/L peroxide led to complete inactivation (i.e. $\leq$2 CFU/mL which is the detection limit) with 11.9 kJ/L at pH 3 and 16.9 kJ/L at pH 4–8, but no mineralization occurred. When the process was added 5 mg/L Fe^{2+}, complete inactivation required 17.1 kJ/L at pH 3 but this was accompanied by 36% mineralization. Interestingly, doubling the concentration iron and peroxide hindered inactivation but promoted mineralization; these results demonstrate a competitive effect between spores and the effluent organic matter for hydrogen peroxide, hydroxyl radicals and other ROS and highlight the importance of the nature of the microorganism. Finally, the implications for wastewater treatment are also discussed.

1. Introduction

Wastewater has been used as a source of crop nutrients over decades with a long tradition in developing countries like China, Mexico, Peru, Egypt, Lebanon, Morocco, India and Vietnam [1]. Although there is not any available database, it is estimated that more than 4–6 million ha are irrigated with wastewater or polluted water [1]. According to the World Health Organization, about 20 million ha worldwide are irrigated with wastewater or polluted water; this corresponds to nearly 7% of the total irrigated land [2].

In developed countries, water recycle and reuse aim at (i) managing the physical water scarcity (including climate change and drought management), (ii) achieving water reallocations from agriculture to other uses, and (iii) becoming an economic response to costly inter-basin transfers [1]. Depending on the final water reuse and given that wastewater is often polluted by toxic or non-biodegradable organic compounds and pathogens, different quality limits have been established for drinking water and irrigation water of crops.

Fusarium genus has been found to be one of the most common occurring microorganisms which severely affect a wide variety of crops. This genus is a filamentous fungus commonly found in soil and it can be worldwide spread through water. It has high detrimental impact on crop production globally [3]. Our previous contributions showed that *Fusarium* is a good model phytopathogen due to its high resistance to standard water disinfection practices [4,5] and its negative effect over humans [6].

Due to the presence of these resistant species in wastewaters, it is important to look for efficient treatments as alternatives to the traditional processes used in municipal wastewater treatment plants. Advanced oxidation processes (AOPs), have been considered recently as a promising option for water treatment in these cases. The efficacy of AOPs is due to the high capacity of hydroxyl radicals ($OH^{\bullet}$) to oxidize almost all organic compounds, since these radicals are very powerful oxidants as they are non-selective and highly reactive. The use of several AOPs for water disinfection purposes has awakened the interest of researchers recently [7–9]. Among the AOPs used for water disinfection, photocatalysis with UV-irradiated titanium dioxide has been the most studied. Nevertheless, the interest to the application of other powerful oxidative treatments has increased in the field of solar water disinfection, especially H_2O_2/UV–vis and the photo-Fenton processes.

* Corresponding author. Tel.: +34 950 387957; fax: +34 950 363015.
E-mail address: pilar.fernandez@psa.es (P. Fernández-Ibáñez).

0926-3373/$ – see front matter © 2011 Elsevier B.V. All rights reserved.
doi:10.1016/j.apcatb.2011.11.006

The efficacy of the photo-Fenton process can be explained by the increased amount of OH• generated through the catalytic cycle of iron ions (Fe^{2+} and Fe^{3+}) combined with H_2O_2 and UV–vis photons. The main reactions involved in Fenton process are described as follows [10]:

$$Fe^{2+} + H_2O_2 \rightarrow Fe^{3+} + OH^- + OH^\bullet \ (K = 70\ M^{-1}\ s^{-1}) \quad (1)$$

$$Fe^{3+} + H_2O_2 \rightarrow Fe^{2+} + HO_2^\bullet + H^+ \ (K = 1\text{–}2 \times 10^{-2}\ M^{-1}\ s^{-1}) \quad (2)$$

$$OH^\bullet + H_2O_2 \rightarrow HO_2^\bullet + H_2O \ (K = 1.7\text{–}4.5 \times 10^{-7}\ M^{-1}\ s^{-1}) \quad (3)$$

$$OH^\bullet + Fe^{2+} \rightarrow Fe^{3+} + OH^- \ (K = 3.2 \times 10^{8}\ M^{-1}\ s^{-1}) \quad (4)$$

$$Fe^{3+} + HO_2^\bullet \rightarrow Fe^{2+} + O_2 + H^+ \ (K = 1.2 \times 10^{6}\ M^{-1}\ s^{-1}) \text{ at pH 3} \quad (5)$$

$$Fe^{2+} + HO_2^\bullet + H^+ \rightarrow Fe^{3+} + H_2O_2 \ (K = 1.3 \times 10^{6}\ M^{-1}\ s^{-1}) \text{at pH 3} \quad (6)$$

$$HO_2^\bullet + HO_2^\bullet \rightarrow H_2O_2 + O_2 \quad (7)$$

The OH• production is highly increased by UV–vis irradiation up to a wavelength of 600 nm [7]:

$$Fe(OH)^{2+} + h\nu \rightarrow Fe^{2+} + OH^\bullet \quad (8)$$

After photo-dissociation of Fe^{3+} complexes, ferrous ions are regenerated and re-initiate the Fenton reaction (Eq. (1)), thus closing the photo-catalytic cycle and leading to hydroxyl radicals generation, while eliminating the need for further addition of iron. This catalytic cycle is strongly dependent on pH due to the hydroxyl complex formed by iron dissolved in water ($Fe(OH)^{2+}$). It is widely accepted that the optimum pH for photo-Fenton application is 2.8 [10]. However, this process is even more complex when water also contains organic and inorganic compounds. This is the case of wastewater, where some molecules may be scavengers of hydroxyl radicals. It is well known the detrimental effects of inorganic ions like HCO_3^-, SO_4^{2-}, Cl^-, HPO_4^{2-} and NO_3^- on photo-Fenton efficiency. This fact has been previously reported in the literature for different contaminants like dyes, pesticides and pharmaceutical derivates [7,11,12].

Over the past several years, there has been a growing interest in the application of solar photo-Fenton for water disinfection, with *Escherichia coli* being the most widely investigated bacterium. Pulgarin and co-workers showed that the inactivation of *E. coli* under sunlight could be enhanced adding Fe^{2+} or Fe^{3+} and H_2O_2. They also showed that some organic and inorganic molecules in the water matrix were responsible for the reduced disinfection efficiency of photo-Fenton [8,9]. Not only bacteria but other types of microbial contaminants, like prions and phages have been also evaluated under photo-Fenton. Paspaltis et al. [13] showed that photo-Fenton could efficiently degrade recombinant prions proteins using low amounts of iron (i.e. 12 μg/mL Fe^{3+} in the presence 500 μg/mL H_2O_2). MS2 bacteriophages were also inactivated in water using Fenton and photo-Fenton processes [14,15]. However, this treatment has not yet been applied to evaluate the inactivation efficiency of phytopathogenic fungi under natural sunlight.

When studying solar photo-Fenton, the solar H_2O_2/UV–vis process must be also taken into account. The dissociation of one molecule of hydrogen peroxide under UV photons (Eq. (9)) to generate two OH• takes place at wavelengths below 300 nm [16,17], but this range of UV is not achieved on the earth's surface:

$$H_2O_2 + h\nu \rightarrow 2OH^\bullet \quad (9)$$

H_2O_2 is a required additive for photo-Fenton reactions, and it can be used as a good disinfectant along with ozone or UVC lamps [5,7]. However, the photo-assisted disinfection of water using just H_2O_2 combined together with near UV or visible light has been reported in literature for *E. coli* [18]. More recently, this process (with low amounts of hydrogen peroxide added) has been also reported as a good technique for the disinfection of water polluted with *Fusarium* spores [5,19].

This paper reports on the efficiency of solar photo-Fenton reaction and solar H_2O_2/UV–vis to disinfect simulated municipal effluents (characterized by a pH of about 8 with 25 mg/L of dissolved organic carbon (DOC) and 66 mg/L of inorganic carbon) polluted with *F. solani* spores in solar bottle reactors under natural solar conditions. Due to the combination of several factors playing a key role in the spore inactivation process and due to the presence of organic and inorganic compounds in the water, the spore inactivation rate and DOC reduction were evaluated at different pH values, i.e. 3, 4, 5 and 8. Moreover, the implication of the spores germination in the water under sunlight on the photocatalytic treatment efficiency has been studied.

2. Materials and methods

2.1. Fungi genus quantification

A wild strain of *Fusarium solani* has been used in this experimental work. It was isolated from rainfall over the Andarax River in Almeria (Spain) by researchers in the Department of Plant Production of the University of Almeria. This genus has been used as target to evaluate different solar disinfection treatments in our previous research [4,5,19,20]. This genus is producer of microconidia spores, which were grown on acidified malt agar plates and recovered by washing them with distilled water. Spore concentration was determined by direct counting with a Neubauer plate (Brand, Germany) with a model Eclipse 50i Nikon (Japan) optical microscope, and diluted in the reactor to the desired spore concentration, in this experiment 10^3 CFU/mL. Spore concentration in water samples during solar tests was measured using the plate counting technique. 50–250–500 μL of the sample were plated out on acidified malt agar (Sigma Aldrich, USA) to reach the 2 CFU/mL detection limit (DL). Samples and analyses were replicated three times. The plates were incubated for 2 days at 28 °C in the dark before counting. A one-way ANOVA ($P < 0.05$, confidence > 95%, Origin v7.03, OriginLab Corp., Northampton, USA) of results reported a 95% confidence level for the average colony concentration and error.

Recover (or regrowth) counts of fungi spores were determined for all experiments by leaving the last two samples at room temperature for a week. The same plate counting method was used to determine spores counts. No spore re-growth was observed in any case when the final sample achieved detection limit.

2.2. Simulated municipal wastewater treatment plant effluent

A simulated municipal wastewater treatment plant effluent (SMWWE) containing 25 mg/L of DOC was employed in this work. The exact composition is as follows: $NaHCO_3$ (96 mg/L), NaCl (7 mg/L), $CaSO_4{\cdot}2H_2O$ (60 mg/L), urea (6 mg/L), $MgSO_4$ (60 mg/L), KCl (4 mg/L), K_2HPO_4 (0.28 mg/L), $CaCl_2{\cdot}2H_2O$ (4 mg/L), peptone (32 mg/L), $MgSO_4{\cdot}7H_2O$ (2 mg/L) and meat extract (22 mg/L). Table 1 shows the main physicochemical properties of SMWWE used in the experiments. The natural pH of this water is around 8. DOC and dissolved inorganic carbon (DIC) were measured by direct injection of samples filtered with 0.2 μm syringe-driven filters into a Shimadzu – 5050A TOC analyzer.

2.3. Solar bottle reactor

The experiments were performed in 250 mL DURAN-glass (Schott, Germany) batch bottle reactors, which were described elsewhere [4,5,19,20]. The total volume of irradiated water is

Table 1
Physicochemical properties of SMWWE used in this work.

	SMWWE		SMWWE
Cl^-	11.6 mg/L	Na^+	33.3 mg/L
NO_3^-	0 mg/L	Mg^{2+}	17.8 mg/L
SO_4^{2-}	93.9 mg/L	K^+	15.3 mg/L
NH_4^+	1.16 mg/L	Ca^{2+}	34.5 mg/L
PO_4^{3-}	0.51 mg/L	HCO_3^-	64.4 mg/L
Turbidity	1.5 NTU	pH	8.15
Bacteria	2 CFU/mL	Conductivity	362 μS/cm

200 mL with 0.0095 m^2 of irradiated surface. All the experiments were conducted at Plataforma Solar de Almeria (PSA). The reagents and spore suspensions were added to water and then stirred at 100 rpm throughout the experiment to obtain a homogeneous suspension. Afterwards, the bottles were covered with a glass cap to allow the solar radiation to enter the bottle-reactor from all directions, and exposed to sunlight for 5 h (10:30–15:30, local time) on completely sunny days. Time required to complete the experiment lasted from September 2010 to January 2011. All experiments were performed in triplicate (three bottles per treatment). The results of all three repetitions were highly reproducible. The first sample of each experiment was kept in the dark at room temperature and analyzed again at the end of the experiment to exclude any effects of the reaction in the dark. Temperature (Checktemp, Hanna instruments, Spain), dissolved oxygen (DO) and pH (multi720, WTW, Germany) were measured directly in the bottle reactor during the experiments. To acidify the water solutions, sulfuric acid (Merk, Germany, analytical grade) was used.

2.4. Solar radiation

A solar energy unit, Q_{UV}, is a term commonly used to compare results under different solar irradiation conditions [21]. Q_{UV} estimates the accumulated UV energy in the photoreactor per unit volume of treated water for a given time during the experiment. This factor permits to normalize the energy available for the photocatalytic reaction under natural sunlight. The intensity of the solar UV irradiation was measured with a global UVA radiometer (295–385 nm, Model CUV3, Kipp & Zonen, Netherlands) with a typical sensitivity of 264 mV/(W m^2), which provides data in terms of incident W/m^2. This is used to calculate the total UV energy received per unit volume according to Eq. (10) [21]:

$$Q_{UV,n} = Q_{UV,n-1} + \frac{\Delta t_n \overline{UV}_{G,n} A_r}{V_t} \quad \Delta t_n = t_n - t_{n-1} \tag{10}$$

where $Q_{UV,n}$, $Q_{UV,n-1}$ is the UV energy accumulated per unit volume (kJ/L) at times n and $n-1$, respectively, $UV_{G,n}$ is the average incident irradiation on the irradiated area, Δt_n is the experimental time of sample, A_r is the illuminated area of collector (m^2), and V_t is the total volume of treated water (L).

2.5. Analysis of iron concentration

Ferrous sulfate heptahydrate ($FeSO_4 \cdot 7H_2O$, PANREAC, Spain) was used as the source of Fe^{2+} at concentrations of 5 mg/L and 10 mg/L. Water samples were filtered with NY 0.2 μm CHROMAFIL® Xtra PET-20/25 (PANREAC, Spain) to remove precipitated iron. After that, each sample was mixed with 1 mL of 1,10-fenantroline (1 g/L) and 1 mL of buffer solution according to ISO 6332 to measure the Fe^{2+} and total iron (Fe^{tot}) concentration. Then, the coloured complex formed was measured with a spectrophotometer (PG Instruments Ltd T-60-U) at 510 nm in glass cuvettes (1 cm path length). Fe^{2+} and Fe^{tot} were determined using corresponding calibration curves. The concentration of Fe^{3+} was determined subtracting Fe^{2+} from Fe^{tot}. The molar ratio of iron to H_2O_2 used was 1:2.

2.6. Analysis of H_2O_2 concentration

Hydrogen peroxide (30%, w/v aqueous solution) was provided from Riedel-de Haën (Germany) and diluted directly into the reaction mixture. 10 mg/L was used to perform the H_2O_2/UV–vis and the photo-Fenton experiments, the concentration was chosen based on previous results where a higher concentration did not increase the inactivation rate [4]. H_2O_2 concentration was measured in a spectrophotometer (PG Instruments Ltd T-60-U) at 410 nm in glass cuvettes (1 cm path length) according to DIN 38409 H15 based on the formation of a yellow complex from the reaction of titanium (IV) oxysulfate with H_2O_2. The titanium (IV) oxysulfate method has a 0.1 mg/L detection limit. The signal was read after 5 min incubation time against a H_2O_2 standard curve linear in the 0.1–100 mg/L H_2O_2 concentration range. The titanium (IV) oxysulfate solution (Riedel-de Haën, Germany) was used as received.

3. Results and discussion

3.1. Dark Fenton experiments

Fig. 1a shows the behavior of *Fusarium* spore in SMWWE under dark Fenton with 5 mg/L Fe^{2+} and 10 mg/L H_2O_2 at pH 3 (best conditions for Fenton reaction) during 5 h. The initial microconidia concentration of 10^3 CFU/mL remained constant for 5 h of treatment, demonstrating that the dark Fenton reaction does not impose a detrimental effect on the spores, and neither does the acidic pH of the water nor the temperature, which varied from 23 °C to 25 °C. Table 2 shows the pH, DO and DOC of water at the beginning and after 5 h of oxidation. Previous findings [19] showed that fungal viability is unaffected by temperatures below 40 °C, therefore thermal inactivation of fungal spores was discarded during the experiments.

Water pH remained constant during the experiment at pH 3. DOC decreased slightly by about 8%, from 26.0 (±0.5) mg/L to 23.9 (±0.7) mg/L. Fe^{2+}, Fe^{3+}, Fe^{tot} and H_2O_2 were also monitored throughout the experiment (Fig. 1b). Total dissolved iron (Fe^{tot}) was 5 mg/L (same concentration as initially added) and it remained constant during the experiment, while the amount of hydrogen peroxide consumed was 4.8 mg/L after 5 h of treatment.

The $OH^\bullet$ radicals generated during the dark Fenton reaction have been proven ineffective to inactivate microconidia of *F. solani*, showing the strong resistance of this spore. The main reaction involved in Fenton process is Eq. (1) where the Fe^{2+} combined with H_2O_2 is rapidly oxidized to Fe^{3+} and $OH^\bullet$ radicals are generated. This fast reaction leads to the accumulation of Fe^{3+} in the water and fast consumption of $OH^\bullet$ during the treatment. This justifies why most of Fe^{tot} measured in the water is Fe^{3+} (Fig. 1b). The absence of light limits Fe^{2+} regeneration (Eq. (8)), and the catalytic cycle is, therefore, limited. For this reason, the dark Fenton reaction cannot be employed as a disinfection method at the conditions of this study.

3.2. Influence of pH on solar disinfection

Fig. 2 shows the effect of pH on the inactivation of *F. solani* microconidia under natural solar irradiation. Experiments were performed at the SMWWE's inherent pH (8), as well as at acidic conditions (pH 3 and 4) to allow for a better comparison with the respective runs in the presence of iron and/or H_2O_2 that were carried out in the same pH range. As clearly seen, solar irradiation achieved only partial disinfection with the effect of pH being inconsiderable; for example, the spore concentration decreased from approximately 1000 CFU/mL to 152 (±13) CFU/mL,

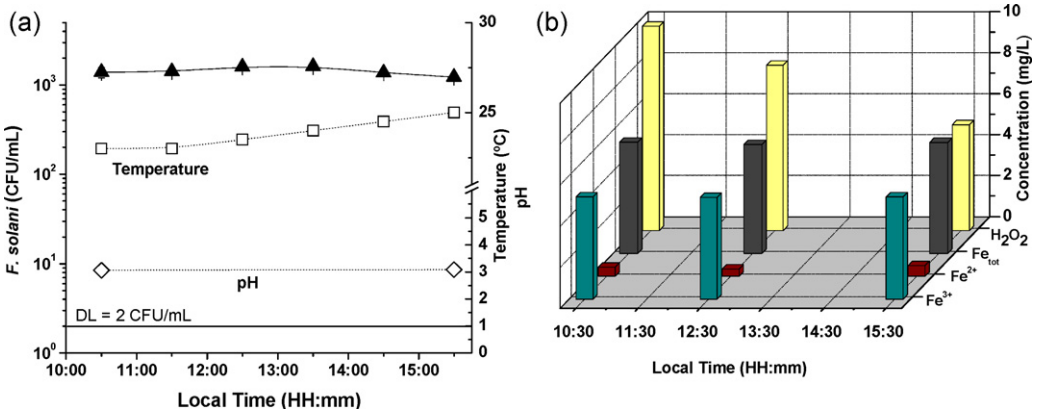

Fig. 1. (a) *F. solani* microconidia concentrations in SMWWE for 5 h of dark Fenton treatment with 5 mg/L Fe^{2+} and 10 mg/L H_2O_2 (-▲-). Temperature and pH are shown with dashed lines. (b) Evolution of H_2O_2, Fe^{2+}, Fe^{3+} and Fe^{tot} concentrations during the experiment. DL = 2 CFU/mL.

134 (±5) CFU/mL and 111 (±17) CFU/mL after 5 h of solar exposure at 21.1 kJ/L and pH of 8, 4 and 3, respectively.

DOC remained unchanged under solar disinfection (Table 2). The maximum temperature achieved during the experimental time was 37.6 °C and pH remained constant. Moreover, the pH effect alone was also studied in dark and it was found that pH 3 did not affect the spore viability after 5 h (data not shown) which implies that acidic conditions alone are not capable of killing *F. solani*. Hence, it can be hypothesized that spore inactivation under sunlight is due only to the synergistic effect between the temperature and the intensity of solar irradiation.

The main mechanisms involved in the inactivation process under natural sunlight are (i) the accumulation of DNA mutations provoked by UVA irradiation, and (ii) the oxidative stress induced by reactive oxygen species (ROS) generated in the water under UVA irradiation [22–24]. The main mutagenic DNA lesions are cyclobutane-pyrimidine dimers (CPDs), which are also the most abundant and cytotoxic after the UV exposure [25]. 6–4 Photoproducts (6–4 PPs, which are pyrimidine adducts) are also generated and may be even more lethal and mutagenic. Both types of products generated by UV irradiation distort the DNA helix; if these lesions remain unrepaired, a single CPD is enough to inhibit the gene and stop the transcription and replication activity leading to misreading of the genetic code causing mutations and eventually cells' death [25]. Cells damage can occur also by the oxidative attack of ROS like the superoxide anion (O_2^-), hydrogen peroxide, etc. which are generated also under background levels of sunlight irradiation [26]. When ROS interact with DNA, single strand cleavages occur as well as nucleic base modifications which may have lethal and mutagenic consequences. Furthermore, oxidation of proteins and membrane damage is also induced under UVA exposure [24]. Another possible way of damage will include the internal photo-Fenton reaction assisted by the iron inherently existing in the microorganisms [9].

At the conditions employed in this study, the inactivation of *F. solani* was not complete (i.e. down to detection limit) presumably due to the fact that the applied UV dose was inadequate. Similar results were obtained by Sichel et al. [20,27] with several *Fusarium* species. They found that the disinfection of spores was strongly influenced by the sunlight dose accumulated during the experiment, while they reported that a solar UV dose of 8 kJ/L was needed to achieve complete disinfection in distilled water [20,27].

3.3. H_2O_2/UV–vis at different pH values

The effect of changing pH in the range 3–8 on the performance of the H_2O_2/UV–vis process was examined and the results are summarized in Fig. 3 and Table 2. As clearly seen, inactivation of *F. solani* to the detection limit was achieved after 11.9 kJ/L of Q_{UV} and

Table 2
Initial (i) and final (f) values of pH, DO and DOC for all experiments. The last column shows if the detection limit (DL = 2 CFU/mL) was reached at any time of the experiment (YES or NO). Q_{UV} shows the accumulated solar UV irradiation per unit volume either at the moment where the detection limit was achieved or at the end of the experiment.

	pH_i	pH_f	DOC_i, mg/L	DOC_f, mg/L	DOC reduction (%)	DO_i, mg/L	DO_f, mg/L	Q_{UV}, kJ/L	DL
Dark Fenton (5 mg/L Fe^{2+} to 10 mg/L H_2O_2)									
pH 3 (Fig. 1)	3.1	3.1	26.0 ± 0.5	23.9 ± 0.7	8.2	7.3	7.1	0	NO
Solar disinfection									
pH 8 (Fig. 2)	7.8	8.3	26.5 ± 0.1	27.6 ± 0.1	0	6.9	6.9	21.1	NO
pH 4 (Fig. 2)	4.1	4.2	26.5 ± 0.1	26.5 ± 0.1	0	6.7	7.1	21.1	NO
pH 3 (Fig. 2)	3.07	3.15	26.5 ± 0.1	26.6 ± 0.1	0	6.8	7.2	21.1	NO
H_2O_2/UV–vis (10 mg/L H_2O_2)									
pH 8 (Fig. 3)	8.2	8.5	26.6 ± 0.4	27.1 ± 0.5	0	7.1	7.1	16.9	YES
pH 4 (Fig. 3)	3.8	3.9	23.6 ± 0.1	22.8 ± 1.2	0	7.3	7.2	16.9	YES
pH 3 (Fig. 3)	3.1	3.1	24.0 ± 0.1	23.4 ± 0.9	0	7.3	6.3	11.9	YES
Photo-Fenton (5 mg/L Fe^{2+} to 10 mg/L H_2O_2)									
pH 8 (Fig. 5)	7.3	8.2	25.2 ± 0.1	22.3 ± 0.3	11.8	7.30	6.32	21.1	NO
pH 5 (Fig. 5)	4.9	4.4	25.5 ± 0.5	20.9 ± 0.5	17.8	7.30	6.87	19.3	YES
pH 4 (Fig. 5)	4.0	3.9	27.1 ± 0.5	21.9 ± 0.8	19.0	7.33	6.85	17.4	YES
pH 3 (Fig. 5)	3.1	3.2	26.5 ± 0.1	17.0 ± 2.0	35.5	7.03	6.55	17.1	YES
Photo-Fenton (10 mg/L Fe^{2+} to 20 mg/L H_2O_2)									
pH 5 (Fig. 6)	4.9	3.8	26.1 ± 0.5	18.2 ± 0.5	30.2	7.08	7.01	15.1	NO
pH 4 (Fig. 6)	4.0	3.6	26.1 ± 0.5	17.1 ± 0.7	34.8	7.13	6.98	15.1	NO
pH 3 (Fig. 6)	3.1	3.3	22.4 ± 0.5	5.4 ± 0.6	75.9	6.56	5.88	13.9	NO

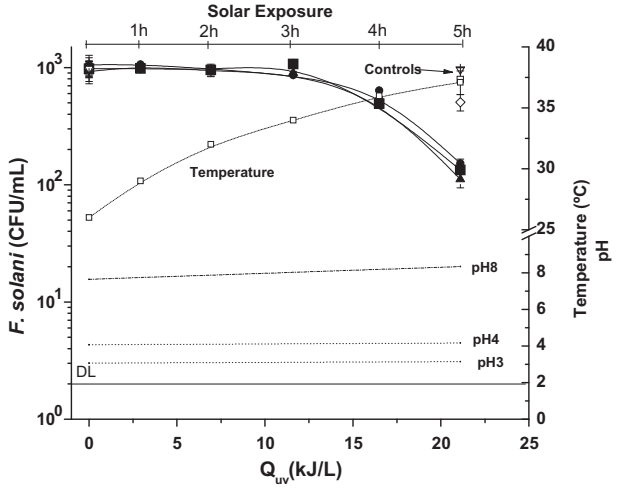

Fig. 2. Solar disinfection of *F. solani* microconidia in SMWWE under natural sunlight at pH 3 (-▲-), pH 4 (-■-) and pH 8 (-●-) as a function of Q_{UV}. Each point represents the average of three replicates and error bars the error at a 95% confidence level. Temperature and pH are shown with dashed lines. DL = 2 CFU/mL.

3 mg/L of H_2O_2 consumed at pH 3 and an initial concentration of 936 (±194) CFU/mL. The required UV dose to achieve the detection limit increased to 16.9 kJ/L at pH 4 or 8, whereas the respective H_2O_2 consumption was 2.3 and 1.9 mg/L, respectively.

Regardless the initial pH of the reaction mixture, DOC remained practically unchanged after 5 h of treatment and so did the starting pH value. Temperature increased from 26 °C to 38.4 °C during solar tests. Since *Fusarium* spores viability is not affected by temperatures below 40 °C [4,19,27,28] and increased temperatures were reached when the spore inactivation process had already been started (see Fig. 3), inactivation due to thermal effects can safely be disregarded. Interestingly, the concentration of H_2O_2 needed to inactivate the spores at inherent pH was about 35% lower than that at pH 3 although the required UV dose was about 40% higher.

To assess whether disinfection is due to the combined effect of hydrogen peroxide and sunlight rather than to the presence of 10 mg/L peroxide alone, experiments were performed in the dark at various H_2O_2 concentrations. No inactivation of *Fusarium* spores was observed at concentrations lower than 50 mg/L, while poor and slow inactivation was recorded in the range 50–500 mg/L H_2O_2; only at concentrations greater than 500 mg/L, did inactivation increase to acceptable levels as reported in a previous work of our group [5].

A comparison of the evolution of spores' viability shown in Figs. 2 and 3 shows the strong disinfection capacity of sunlight together with a relatively low amount of added hydrogen peroxide. It must be underlined that these spores are strongly resistant at acidic pH values (e.g. they remain cultivable at pH values as low as 2 and conditions of high salinity), as well as to chlorine and even UV lamps [5]. On the other hand, the dark Fenton experiments (Fig. 1) demonstrated that the concentration of reagents used in this work did not affect the *F. solani* microconidia viability, thus the spore inactivation recorded in Fig. 3 is clearly a result of the synergistic effect between H_2O_2 and sunlight.

The synergistic bactericidal effect of hydrogen peroxide and sunlight has been reported for *E. coli* [9,18,22] and, more recently, for *Salmonella* sp [29]. In a previous work of ours, coupling solar light with H_2O_2 (10 mg/L) was capable of inactivating chlamydospores of *F. equiseti* in distilled water, well water and simulated wastewater [4]. In this study, the efficient inactivation of *F. solani* spores in simulated wastewater added with 10 mg/L H_2O_2 and irradiated by natural sunlight is reported.

The photo-inactivation of spores in the presence of H_2O_2 may be explained through the following two mechanisms:

(i) The generation of ROS alongside DNA mutations induced by the direct action of the sunlight, which yields only a slight reduction in the spore concentration (Fig. 2).

(ii) The involvement of internal Fenton and Haber–Weiss reactions. This mechanism occurs due to the fact that H_2O_2 is uncharged and it can penetrate through cells' membranes and diffuse into the cell. This increases intracellular H_2O_2, which reacts with free iron or loosely bound iron from iron sources like sulfur cluster, proteins such as enterobactin or ferritin and biosynthesized siderophores or Fe-transport siderophores. The intracellular reaction between hydrogen peroxide and 'free-iron' generates $OH^{\bullet}$ via Haber–Weiss reaction. This mechanism has been widely explained by other authors for *E. coli* [9] and *F. equiseti* chlamydospores [4].

It is also notable that DOC remained unchanged during experiments with H_2O_2/UV–vis (unlike what happens during photo-Fenton experiments as this will be discussed in Section 3.4); this supports the theory of the spores undergoing an internal photo-Fenton process as generated $OH^{\bullet}$ did not attack the organic matter dissolved in the water.

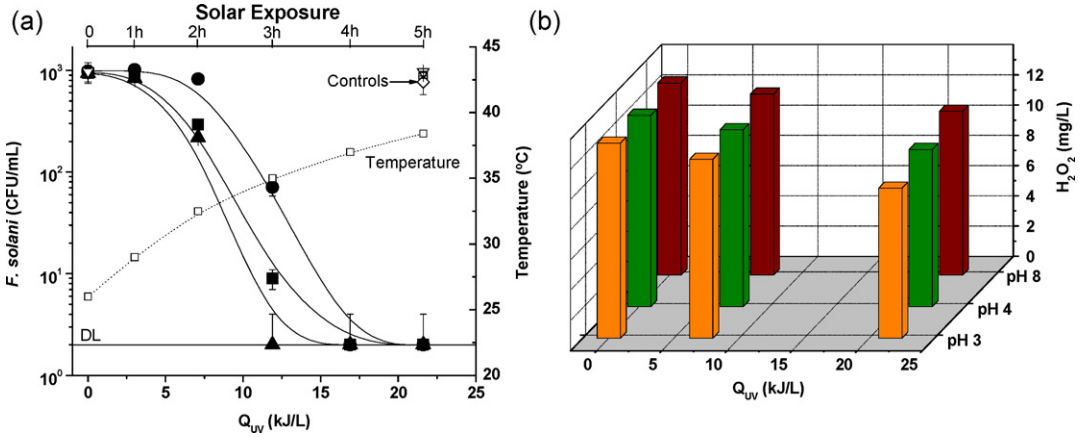

Fig. 3. (a) *F. solani* inactivation under natural solar irradiation with 10 mg/L H_2O_2 at pH 3 (-▲-), pH 4 (-■-) and pH 8 (-●-) in SMWWE as a function of Q_{UV}. Temperature is shown with dashed line. (b) Evolution of H_2O_2 concentration during the experiment. DL = 2 CFU/mL.

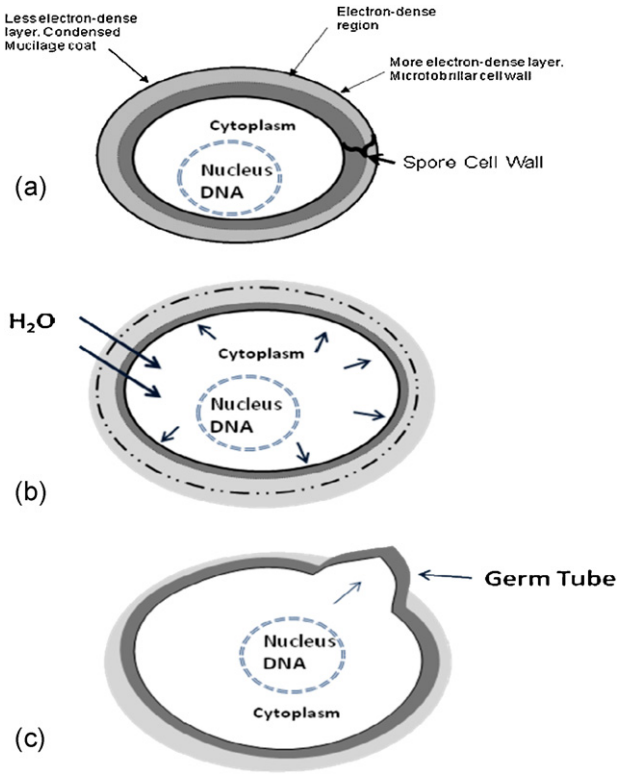

Fig. 4. The various stages of spore germination. (a) Ungerminated conidia (adapted from [35]); (b) spore swelling and first stage of spore germination. (c) Germ tube development (adapted from [34]).

The spores used in this work have a different nature in comparison to bacteria cells. They are microbiological structures designed to survive under strong environmental factors of stress, having a thick, double cell wall protecting themselves against external factors. These structures complete their living cycle by germination and growth. The germination step only occurs under favorable environmental conditions like ideal temperature, exposition to sunlight and into aqueous media containing organic carbon substrates (sugars, alcohols, amino acids) and inorganic salts which provide a more suitable environment for germination [30–33]. During germination spores swell and as a result the size of the spore increases and the enzymatic/metabolic activity is activated. Finally, the mycelium of the fungi will grow through the formation of the germination tube. This process has been widely studied [34,35] and is schematically shown in Fig. 4.

During solar experiments, the first step of spore germination (swelling) will initiate after a certain period of exposition to sunlight (i.e. tens of minutes) with water – and all dissolved compounds – entering into the spore; this is the most important fact to explain the mechanism of the disinfection process since it explains how hydrogen peroxide enters the spore and why inactivation does not start until spores have time to initiate swelling.

Solar irradiation produces damages over the microorganisms. Depending on the solar UV dose received by the microorganisms, these damages can be more or less serious, even leading to cell death. The case of spores is different from that of bacteria, because they do not activate their metabolic activity until germination is initiated and their external wall is more robust and resistant than that of bacteria. For this reason, the solar UV doses required to inactivate aqueous suspensions of spores are much higher than those needed for bacteria. We previously demonstrated [20,27] that mere action of solar irradiation is not as efficient for disinfection of water polluted with fungal spores as for bacterial contamination. This work also shows that long exposure to natural solar irradiation (regardless of the pH) does not produce enough damages over spores to achieve complete reduction of spore concentration to the detection limit.

When hydrogen peroxide is used together with solar photons a strong synergy is observed. This can occur only because spores assimilate H_2O_2 molecules during swelling and in the presence of solar photons a series of reactions permit hydroxyl radicals generation through Haber–Weiss reaction in the presence of intracellular iron. Due to the short life of the $OH^\bullet$ radicals, this mechanism is only possible if the hydroxyl radicals are generated with metal ions bound upon or very closely to the DNA [36]. The fungi spore (as eukaryotic structure) presents an internal cell wall to protect and separate the DNA from the rest of the organelles in the cytoplasm. Thus, $OH^\bullet$ generation by internal photo-Fenton is only possible in the presence of iron or copper in the chromosomes and in the DNA within chromatin molecule [36]. The main product generated by the $OH^\bullet$ attack upon DNA deoxyribose bases is 8-hydroxyguanine produced by the oxidation of guanine bases. Similar products occur with adenine (8-hydroxy adenin) and the pyrimidine bases (cytosine and thymine) which are susceptible to the attack [22,36]. These mechanisms may work together to increase the inactivation rate of *F. solani* microconidia by the H_2O_2/UV–vis process compared to the inactivation obtained with solar irradiation alone.

Taking into account that the spore germination is affected by the pH, it is important to highlight that growing *Fusarium* genus is favored at acidic pH, indeed, the agar used to cultivate the fungi is acidified by citric acid to pH 4 or less [37]. Hence, it can be concluded that the higher spores' inactivation obtained at pH 3 than at pH 8 may be due to the earlier fungi spore activation, with the consequent earlier influx of H_2O_2 into the cells. Furthermore, it is important to consider that during spore germination the internal spore pH, which normally is 6–7 [34], could decrease when the water is taken up by the spore and in the case of pH 3 this could enhance the $OH^\bullet$ production in a similar way of typical photo-Fenton reaction which could explain the results obtained in this work.

The H_2O_2 decomposition rate is influenced by the temperature, UV irradiation, the presence of organic and/or inorganic compounds and the pH of the solution [38]. As all the H_2O_2/UV–vis disinfection experiments were performed simultaneously in the same day, the solar bottle reactors were exposed to identical temperature and UV irradiation, with pH being the only variable factor. Nonetheless, H_2O_2 decomposition in water is not likely to be affected by pH changes in the range 1–9 [39]; therefore, the differences in H_2O_2 consumption recorded in the pH range 3–8 may not be related to the effect of pH on decomposition. However, the initial pH of the effluent may affect the water matrix and, consequently, decomposition. For instance, H_2O_2 could react with carbonates at alkaline conditions as follows [39]:

$$H_2O_2 + CO_3^{\bullet -} \rightarrow HO_2^\bullet + HCO_3^- \quad (11)$$

Reaction (11) is likely to occur at pH 8 but not at pH 3 or 4 where carbonates/bicarbonates would have been reduced to CO_2; therefore, one would expect H_2O_2 consumption at alkaline conditions being greater than that at acidic conditions, which is opposite to what has been found in this work.

Besides the presence of carbonates/bicarbonates, the water matrix contains anions such as sulfates, nitrates, chlorides and phosphates that could partially scavenge H_2O_2, as well as other ROS; the extent of scavenging may depend on the effluent's pH and this would explain the discrepancies in peroxide consumption.

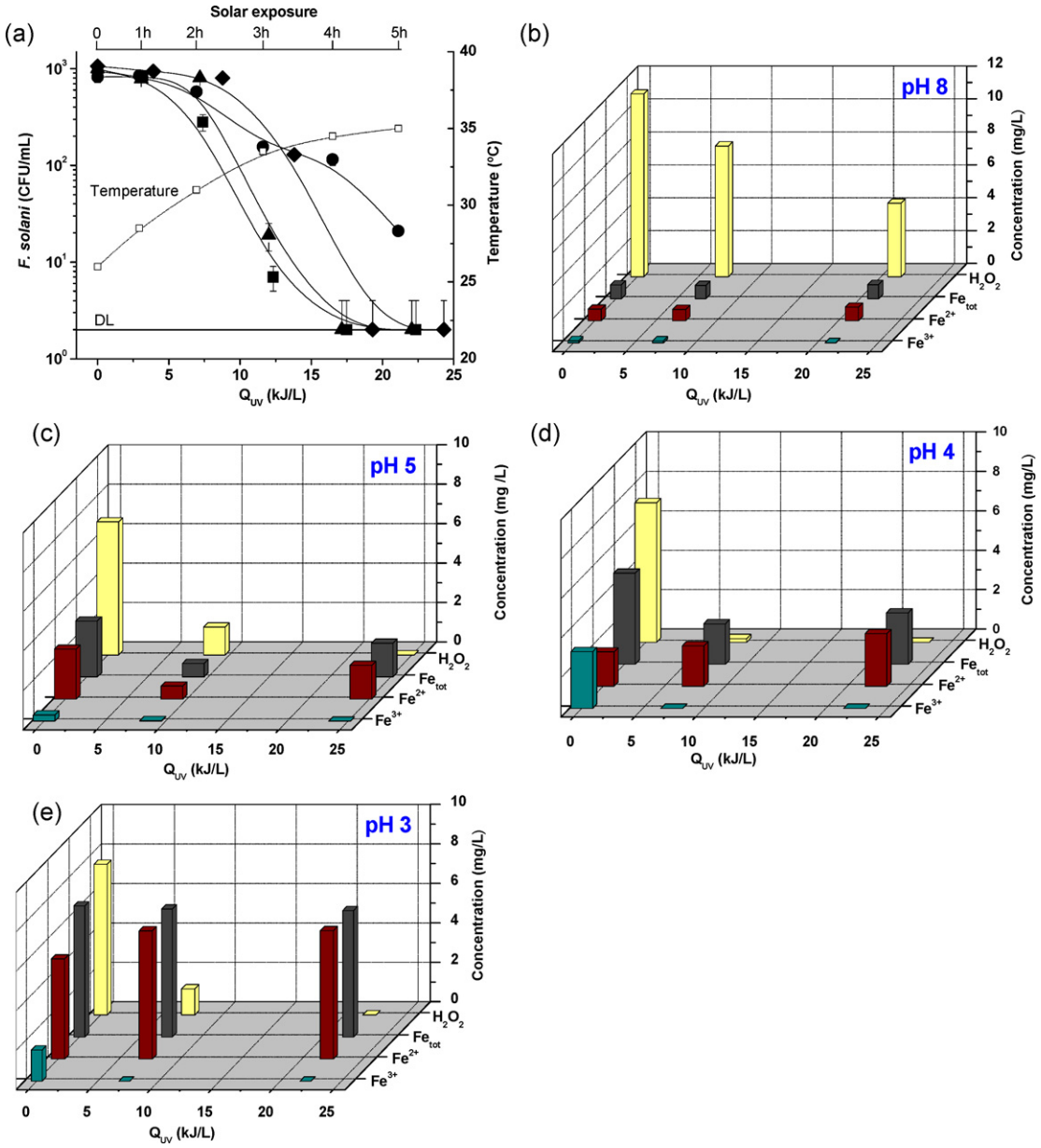

Fig. 5. (a) *F. solani* microconidia inactivation under solar photo-Fenton in the presence of 5 mg/L Fe^{2+} and 10 mg/L H_2O_2 in SMWWE at pH 3 (-▲-), pH 4 (-■-), pH 5 (-♦-) and pH 8 (-●-), as a function of Q_{UV}. Temperature is shown with dashed line. Evolution of H_2O_2, Fe^{2+}, Fe^{3+} and Fe^{tot} concentrations during the experiments performed at (b) pH 8, (c) pH 5, (d) pH 4 and (e) pH 3. DL = 2 CFU/mL.

3.4. Photo-Fenton at different pH values

The effect of varying pH in the range 3–8 on the performance of the photo-Fenton process in the presence of 5 mg/L Fe^{2+} and 10 mg/L H_2O_2 is shown in Fig. 5 and Table 2. As seen, the detection limit 2 CFU/mL was achieved in all cases, except for pH 8.

3.4.1. Photo-Fenton at pH 8

F. solani microconidia concentration decreased from 1060 (±120) CFU/mL to the detection limit (2 CFU/mL) at 21.1 kJ/L (Fig. 5a). Although the initial Fe^{2+} added to the solution was 5 mg/L, the concentration of dissolved Fe^{tot} measured was only 0.8 mg/L, this loss of iron is provoked by the iron precipitation as ferric hydroxide due to the alkaline pH [10]. The amount of hydrogen peroxide consumed after 5 h of treatment was 7.7 mg/L, while the maximum temperature achieved during the process was 36.2 °C. DOC varied from 25.2 (±0.1) mg/L to 22.3 (±0.3) mg/L, which corresponds to about 12% of mineralization.

3.4.2. Photo-Fenton at pH 5

Complete inactivation of *F. solani* spores was achieved, i.e. from an initial concentration of 1060 (±70) CFU/mL to detection limit after 4 h of solar exposure, which corresponds to 19.3 kJ/L of Q_{UV} (Fig. 5a). Fig. 5c shows the evolution of Fe^{tot}, Fe^{2+}, Fe^{3+} and H_2O_2 during the experiment. H_2O_2 was mostly consumed within the first 2 h of solar photo-Fenton treatment. The initial Fe^{tot} dissolved in the water at this pH was 2.9 mg/L, which is higher than that at pH 8 (Fig. 5b). At the end of the experiment, all the dissolved iron was in the form of Fe^{2+}. This is due to the H_2O_2 disappearance at the beginning of the process, which stops photo-Fenton reaction. Therefore, Fe^{2+} could not be transformed to Fe^{3+}, while the light-induced reaction that reduces Fe^{3+} to Fe^{2+} occurs until all iron is transformed into Fe^{2+}. The maximum temperature measured was 35 °C, the pH

dropped from 4.9 to 4.4 and DOC varied from 25.5 (±0.5) mg/L to 20.9 (±0.5) mg/L (i.e. 18% reduction).

3.4.3. Photo-Fenton at pH 4

Fig. 5a shows that spores' inactivation from an initial concentration of 930 (±170) CFU/mL down to the detection limit was reached at 17.4 kJ/L of Q_{UV} for pH 4. The initial Fe^{tot} dissolved in the water was 4.6 mg/L, while H_2O_2 disappeared within the first 2 h of solar treatment (Fig. 5d). Fe^{3+} concentration decreased during the last 3 h due to its reduction to Fe^{2+}, when H_2O_2 was not present in the medium as already explained in Section 3.4.2. At these conditions, inactivation occurred more rapidly than at pH 5 or 8. DOC diminished from 27.1 (±0.5) mg/L to 21.9 (±0.8) mg/L at the end of the experiment, which corresponds to 19% reduction.

3.4.4. Photo-Fenton at pH 3

Photo-Fenton reaction at pH 3 led to complete spores' inactivation (from 1000 (±200) CFU/mL to detection limit) after 4 h of solar exposure, corresponding to 17.1 kJ/L of solar UV energy. Although process performance at pH 3, in terms of inactivation, was similar to that at pH 4, the former exhibited a substantially higher DOC reduction from 27 (±1) mg/L to 17 (±2) mg/L (i.e. 35.5%). This result can be attributed to the high amount of dissolved iron occurring throughout the experiment at pH 3, as clearly seen in Fig. 5e. H_2O_2 was totally consumed during the first 2 h of the experiment; therefore, most of the recorded mineralization percentage might have occurred at the early stages of the process.

Unlike what happened at pH 4 or above where the initial concentration of Fe^{tot} decreased, its concentration remained constant at pH 3. This behavior could be explained by the change of iron speciation in water at different pH, which does not occur at pH 3 because the iron is more stable and soluble at pH 3 than at higher pH values. Although the pH was not controlled during the experiments, its fluctuations were marginal. Similar tendency on iron concentration was observed with measurements done in distilled water (data not shown), therefore, this behavior is not due to the presence of organic matter.

Lower pH values generally promoted the *F. solani* inactivation rate in photo-Fenton treatment (Fig. 5a). The generation of $OH^{\bullet}$ radicals will be enhanced when the Fe^{tot} added to the solution is completely dissolved. It is well-documented that the extent of iron dissolution in water depends strongly on its pH with the most appropriate value for Fenton reactions being at 2.8 [10]. This is reflected in the results shown in Fig. 5b, c, d and e where the initial amount of dissolved iron increases with decreasing pH.

Moreover, the presence of carbonates/bicarbonates at alkaline conditions can impede the efficiency of the process since these species can act as radical scavengers [11]. Eqs. (12) and (13) show the reaction of carbonates/bicarbonates with hydroxyl radicals [38]:

$$OH^{\bullet} + HCO_3^- \rightarrow {}^{\bullet}CO_3^- + H_2O \quad K = 1.5 \times 10^7\ M^{-1}\ s^{-1} \tag{12}$$

$$OH^{\bullet} + CO_2^{2-} \rightarrow {}^{\bullet}CO_3^- + OH^- \quad K = 4.2 \times 10^8\ M^{-1}\ s^{-1} \tag{13}$$

The presence of organic matter could have a positive effect on the microorganism's inactivation kinetics. According to Spuhler et al., the presence of resorcinol during a photo-Fenton reaction for *E. coli* inactivation enhanced the results, as compared with those found without organic matter. They suggested the presence of photo-active Fe^{3+} or Fe^{2+}-resorcinol complexes which may favor the process, although there was no experimental evidence [9].

In general, the organic matter like quenchers, scavengers or other molecules, in the presence of the photo-Fenton reagent, may react with the generated hydroxyl radicals. Some of them, generate carboxylic and dicarboxylic acids which complex with iron to form ligand radicals as shown in the next equation [7,9,10]:

$$Fe^{3+} - (L)_n + h\nu \rightarrow Fe^{2+} - (L)_{n-1} + L_{ox}^{\bullet} \tag{14}$$

Both, Fe^{2+} and radicals can react with O_2 leading to the formation of ROS, and the concomitant reaction of Fe^{2+} with H_2O_2 leading to the regeneration of Fe^{3+} and the production of $OH^{\bullet}$. This way could be specially interesting at pH above 3, where Fe^{3+} tends to precipitate, and Fe^{3+} organo complexes play an important role for the efficiency of photo-Fenton systems at near neutral pH [9].

Although the natural organic matter may benefit the photo-Fenton process, this only occurs in the presence of certain molecules like oxalic acid, carboxylic acids and intermediates. The simulated wastewater used in this study does not contain this kind of compounds. Therefore, we cannot expect a positive effect in the microbial inactivation kinetics as a wide-ranging behavior. Moreover, we did not observe an enhancement due to the organic matter in the spore killing rate for photo-Fenton at pH 8 (Fig. 5). But we observe good disinfection results only if the pH is near the optimal (pH 2.8).

Spore inactivation by means of photo-Fenton appears to occur in two phases (Fig. 5a), namely: the first part corresponds to the early stages of the treatment (up to approximately 5 kJ/L). Due to the high constant rate of Eq. (1), which plays the main role in the photo-Fenton reaction, H_2O_2 is consumed very quickly at the beginning of the solar exposure at acidic pH (Fig. 5c, d and e). Furthermore and focusing on the DOC reduction results, it is clear that the higher efficiency occurred at the lowest pH 3 and it decreased as pH increased. This is due to H_2O_2 being used firstly in the photo-Fenton elimination of organic carbon, so the diffusion inside the spore was inhibited. Thus, the main damage produced by the photo-Fenton reagents was over the external wall during the first 2 h of exposure.

The second part begins after the second hour of solar exposure (Fig. 5a) and lasts until the end of the experiment. This phase accounts for the main decrease in spore concentration, during which there is no H_2O_2 for photo-Fenton reaction. Therefore, the photo-Fenton cycle is stopped in this phase, no hydroxyl radicals are generated, and Fe^{3+} is totally reduced to Fe^{2+} (Fig. 5c, d and e). The large inactivation of spores observed in this phase is a consequence of the damages produced in phase 1. It is well known that most disinfection processes (i.e. solar disinfection, photocatalytic TiO_2 disinfection, etc.) produce a bacterial damage and the effects on bacterial cultivability are observed afterward. Moreover, during this period, the presence of Fe^{2+} in the water could diffuse easily into the cells [40,41] and generate also internal photo-Fenton reactions with H_2O_2 which is always produced during cellular metabolic activity [9]. This may help also the disinfection process in this phase.

3.4.5. Photo-Fenton at higher concentrations of reagents

To assess the effect of Fenton's reagents on process performance, experiments were conducted doubling their initial concentration, i.e. at 10 mg/L Fe^{2+} and 20 mg/L H_2O_2 and the results are summarized in Fig. 6 and Table 2. Although increased levels of catalyst and oxidant had a pronounced beneficial effect on DOC reduction (i.e. it increased from 35.5% at the lower levels to 76% at the higher levels after 5 h of treatment at pH 3), they also introduced a clear detrimental effect on inactivation. This is due to the mechanism of action of photo-Fenton over spores explained in Section 3.4.4. It seems like if there is a kind of competition for hydroxyl radicals by the organic matter and spores, which makes the disinfection to occur at lower rate.

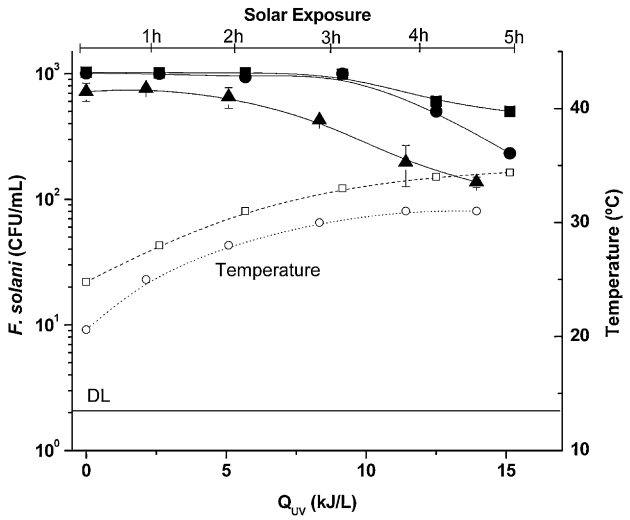

Fig. 6. *F. solani* microconidia inactivation under solar photo-Fenton in the presence of 10 mg/L Fe^{2+} and 20 mg/L H_2O_2 in SMWWE at pH 5 (-■-), pH 4 (-●-) and pH 3 (-▲-) as a function of Q_{UV}. Temperatures are shown with dashed lines for pH 5 and pH 4 (··□··) and pH 3 (··○··). DL = 2 CFU/mL.

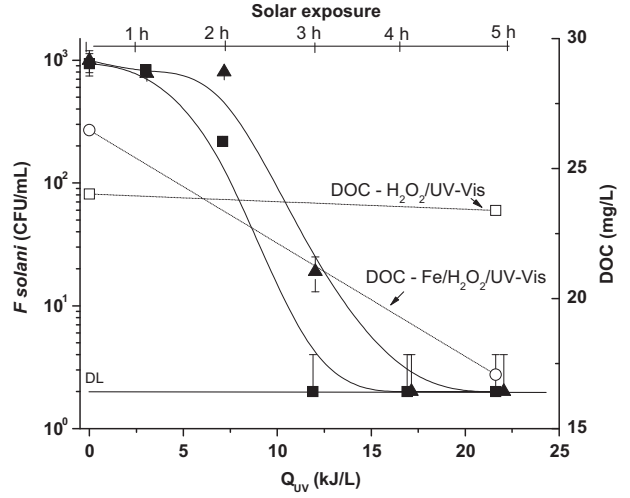

Fig. 7. *F. solani* microconidia inactivation in SMWWE under natural sunlight with 5 mg/L Fe^{2+} and 10 mg/L H_2O_2 at pH 3 (-▲-) or 10 mg/L H_2O_2 at pH 3 (-■-) as a function of Q_{UV}. Same open symbols with dashed lines represent DOC evolution.

3.5. Comparison of H_2O_2/UV–vis and photo-Fenton at pH 3

Fig. 7 shows a comparison between the H_2O_2/UV–vis and photo-Fenton treatments in terms of inactivation and mineralization at pH 3 and a common (10 mg/L) concentration of H_2O_2. Complete inactivation could be achieved in both cases, although the H_2O_2/UV–vis process required less energy (11.9 kJ/L) than the photo-Fenton process (17.1 kJ/L). On the contrary, the latter achieved a substantial DOC removal of 35.5% after 5 h of treatment, while the former resulted in no mineralization.

These findings highlight the importance of the various mechanisms associated with spores inactivation and organic matter degradation. In the case of the H_2O_2/UV–vis system, H_2O_2 penetrates and diffuses in the cell where it induces internal Fenton and Haber–Weiss reactions generating reactive species capable of achieving disinfection. In the case of the photo-Fenton system, it appears that most of the peroxide rapidly decomposes to hydroxyl radicals that preferentially attack the organic matter of the effluent rather than the spores. This competition for both hydrogen peroxide and the secondary oxidants has a contradictory effect; on one hand, it slightly reduces the inactivation rate but, on the other hand, it increases mineralization.

The high inactivation rate of fungi spore with photo-Fenton is also explained by the natural biological cycle of the fungi (Fig. 4). Therefore, the inactivation rate is strongly dependent on the nature of the microorganism under evaluation. This behavior has not been described previously since the photo-Fenton process has been used for organic compounds and bacteria, especially with *E. coli* which presents a low resistance to environmental factors.

4. Conclusions

In this work, the efficacy of solar irradiation coupled with iron ions and/or hydrogen peroxide to inactivate *F. solani* microconidia in synthetic municipal wastewater was evaluated for the first time. The main conclusions drawn from this study are summarized as follows:

1) Unlike bacteria like *E. coli* that are typically employed as test microorganisms to assess the disinfection capacity of AOPs, *F. solani* microconidia are particularly resistant fungal spores that survive at conditions of, e.g. low pH, irradiation in the absence of oxidants or oxidation in the absence of light.
2) Understanding the biology of the microorganism in question is critical to evaluate the disinfection efficiency and mechanisms of the proposed processes. Solar irradiation in the presence of relatively low H_2O_2 concentration (10 mg/L) is capable of inactivating *F. solani* at 11.9–16.9 kJ/L energy dose and this is associated with (i) peroxide diffusing in the cell and initiating internal Fenton and Haber–Weiss reactions, and (ii) photogenerated ROS that also attack the cell.
3) The addition of iron at 5 mg/L to initiate a photo-Fenton reaction retards slightly inactivation (e.g. the required energy is 17.1 kJ/L compared to 11.9 kJ/L without iron at pH 3) but enhances mineralization. This clearly implies a competition between organic matter and the spores for H_2O_2, hydroxyl radicals and other ROS.
4) In this respect, mild photo-Fenton (i.e. relatively low concentrations of reagents and energy (with the latter provided by sunlight)) may be considered as an alternative wastewater treatment technology for the removal of both organic matter and pathogens.

Acknowledgements

Financial support by the Access to Research Infrastructures activity under the 7th Framework Programme of the EU (SFERA Grant Agreement no. 228296) is gratefully acknowledged.

References

[1] P. Drechsel, C.A. Scott, L. Raschid-Sally, M. Redwood, A. Bahri, Wastewater Irrigation and Health, Assessing and Mitigating Risk in Low-Income Countries, International Development Research Centre, Earthscan, London, 2010.
[2] WHO, Guidelines for the Safe Use of Wastewater, Excreta and Greywater, Vol. 2: Wastewater Use in Agriculture, World Health Organization, Geneva, 2006.
[3] E.J. Anaissie, R.T. Kuchar, J.H. Rex, A. Francesconi, M. Kasai, F.C. Müller, M. Lozano-Chiu, R.C. Summerbell, M.C. Dignani, S.J. Chanock, T.J. Walsh, Clin. Infect. Dis. 33 (2001) 1871–1878.
[4] M.I. Polo-López, I. García-Fernández, I. Oller, P. Fernández-Ibáñez, Photochem. Photobiol. Sci. 10 (2011) 381–388.
[5] C. Sichel, P. Fernández-Ibáñez, M. Cara, J. Tello, Water Res. 43 (2009) 1841–1850.
[6] K.M. Old, B. Schippers, Soil Biol. Biochem. 5 (1973) 613–620.
[7] S. Malato, P. Fernández-Ibáñez, M.I. Maldonado, J. Blanco, W. Gernjak, Catal. Today 147 (2009) 1–59.
[8] A.G. Rincón, C. Pulgarin, Appl. Catal. B Environ. 63 (2005) 222–231.
[9] D. Spuhler, J.A. Rengifo-Herrera, C. Pulgarín, Appl. Catal. B Environ. 96 (2010) 126–141.
[10] J.J. Pignatello, E. Oliveros, A. McKay, Crit. Rev. Environ. Sci. Technol. 36 (2006) 1–84.

[11] N. Klamerth, L. Rizzo, S. Malato, M.I. Maldonado, A. Agüera, A. Fernández-Alba, Water Res. 44 (2010) 545–554.
[12] A. Zapata, I. Oller, E. Bizani, J.A. Sánchez-Pérez, M.I. Maldonado, S. Malato, Catal. Today 144 (2009) 94–99.
[13] I. Paspaltsis, C. Berberidou, I. Poulios, T. Sklaviadis, J. Hosp. Infect. 71 (2009) 149–156.
[14] J.I. Nieto-Juarez, K. Pierzchła, A. Sienkiewicz, T. Kohn, Environ. Sci. Technol. 44 (2010) 3351–3356.
[15] J.Y. Kim, C.L. David, L. Sedlak, J. Yoon, K.L. Nelson, Water Res. 44 (2010) 2647–2653.
[16] M.A. Tarr, Chemical Degradation Methods for Wastes and Pollutans: Environmental and Industrial Applications, Marcel Dekker, New York, 2003.
[17] S. Goldstein, D. Aschengrau, Y. Diamant, J. Rabani, Environ. Sci. Technol. 41 (2007) 7486–7490.
[18] P.S. Hartman, A. Eisenstark, J. Bacteriol. 133 (1978) 769–774.
[19] M.I. Polo-López, P. Fernández-Ibáñez, I. García-Fernández, I. Oller, I. Salgado-Tránsito, C. Sichel, J. Chem. Technol. Biotechnol. 85 (2010) 1038–1048.
[20] C. Sichel, J. Tello, M. de Cara, P. Fernández-Ibánez, Catal. Today 129 (2007) 152–160.
[21] P. Fernández, J. Blanco, C. Sichel, S. Malato, Catal. Today 101 (2005) 345–352.
[22] J.A. Imlay, Annu. Rev. Biochem. 77 (2008) 755–776.
[23] E. Ubomba-Jaswa, C. Navntoft, M.I. Polo-López, P. Fernandez-Ibanez, Photochem. Photobiol. Sci. 8 (2009) 587–595.
[24] R.V. Miller, W. Jeffrey, D. Mitchell, M. Elasri, Am. Soc. Microbiol. News 65 (1999) 535–541.
[25] R.P. Sinha, D.P. Häder, Photochem. Photobiol. Sci. 1 (2002) 225–236.
[26] H. Merwald, G. Klosner, C. Kokesch, M. Der-Petrossian, H. Hönigsmann, F. Trautinger, J. Photochem. Photobiol. B: Biol. 79 (2005) 197–207.
[27] C. Sichel, M. de Cara, J. Tello, J. Blanco, P. Fernández-Ibáñez, Appl. Catal. B Environ. 74 (2007) 152–160.
[28] E. Shlevin, Y. Mahrer, J. Katan, Phytopathology 94 (2004) 132–137.
[29] F. Sciacca, J.A. Rengifo-Herrera, J. Wéthé, C. Pulgarin, Chemosphere 78 (2010) 1186–1191.
[30] G.J. Griffin, Can. J. Microbiol. 16 (1970) 733–740.
[31] V.W. Cochrane, J.C. Cochrane, J.M. Vogel, R.S. Coles, J. Bacteriol. 86 (1963) 312–319.
[32] R. Marchant, M.F. White, J. Gen. Microbiol. 48 (1967) 65–77.
[33] D. Palmero Llamas, M. de Cara González, C. Iglesias González, G. Ruiz López, J.C. Tello Marquina, J. Ind. Microbiol. Biotechnol. 35 (2008) 1411–1418.
[34] G.S. Chitarra, P. Breeuwer, F.M. Rombouts, T. Abee, J. Dijksterhuis, Fungal Genet. Biol. 42 (2005) 694–703.
[35] R. Marchant, Ann. Bot. 30 (1966) 441–445.
[36] B. Halliwell, O.I. Aruoma, Chem. Rev. Lett. 281 (1991) 9–19.
[37] H. Okazaki, Ann. Phytopathol. Soc. 41 (1975) 314–320.
[38] C.W. Jones, in: J.H. Clark (Ed.), Applications of Hydrogen Peroxide and Derivates, Royal Chem. Soc., Cambridge, UK, 1999.
[39] C.H. Liao, S.F. Kang, F.A. Wu, Chemosphere 44 (2001) 1193–1200.
[40] R. Tyrrell, C. Pourzand, J. Brown, V. Hejmadi, E. Kvam, S. Ryter, R. Watkin, Radiat. Prot. Dosimetry 91 (2000) 37–39.
[41] A. Imlay, S. Linn, Science 240 (1988) 1302–1309.